BIOCHEMISTRY
including biophysical chemistry & molecular biology
Article

Biochemistry **2010,** *49,* 9613–9619 9613
DOI: 10.1021/bi1011157

Kinetics and Inhibition of Nicotinamidase from *Mycobacterium tuberculosis*†

Derrick R. Seiner, Subray S. Hegde, and John S. Blanchard*

Department of Biochemistry, Albert Einstein College of Medicine, 1300 Morris Park Avenue, Bronx, New York 10461, United States

Received July 13, 2010; Revised Manuscript Received September 27, 2010

ABSTRACT: Nicotinamidase/pyrazinamidase (PncA) is involved in the NAD^+ salvage pathway of *Mycobacterium tuberculosis* and other bacteria. In addition to hydrolyzing nicotinamide into nicotinic acid, PncA also hydrolyzes the prodrug pyrazinamide to generate the active form of the drug, pyrazinoic acid, which is an essential component of the multidrug treatment of TB. A coupled enzymatic activity assay has been developed for PncA that allows for the spectroscopic observation of enzyme activity. The enzyme activity was essentially pH-independent under the conditions tested; however, the measurement of the pH dependence of iodoacetamide alkylation revealed a p*K* value of 6.6 for the active site cysteine. Solvent deuterium kinetic isotope effects revealed an inverse value for k_{cat} of 0.64, reconfirming the involvement of a thiol group in the mechanism. A mechanism is proposed for PncA catalysis that is similar to the mechanisms proposed for members of the nitrilase superfamily, in which nucleophilic attack by the active site cysteine generates a tetrahedral intermediate that collapses with the loss of ammonia and subsequent hydrolysis of the thioester bond by water completes the cycle. An inhibitor screen identified the competitive inhibitor 3-pyridine carboxaldehyde with a K_i of 290 nM. Additionally, pyrazinecarbonitrile was found to be an irreversible inactivator of PncA, with a k_{inact}/K_I of 975 M^{-1} s^{-1}.

Nicotinamidase (PncA)[1] is responsible for the hydrolysis of nicotinamide to nicotinic acid and ammonia in the NAD^+ salvage pathway of *Mycobacterium tuberculosis* and other bacteria (Scheme 1) (*1*). This enzyme is of particular interest because it also hydrolyzes the prodrug pyrazinamide (PZA) to the active bactericidal compound pyrazinoic acid (*2*, *3*). Mutations in the *pncA* gene of *M. tuberculosis* have been shown to generate clinical resistance to PZA (*4*−*7*). PZA, in combination with rifampicin and isoniazid, is the current short course treatment for tuberculosis recommended by the World Health Organization (*3*, *8*). The addition of PZA to this regimen leads to a significant reduction in the length of chemotherapy, from ≥9 to 6 months (*3*). PZA has been shown to inhibit *M. tuberculosis* fatty acid synthetase type 1 and disrupt both membrane function and acidification of the cytoplasm, although its exact mechanism of bactericidal activity still remains unclear (*3*, *9*).

Recent studies have shed light on the biochemical activity (*8*) as well as the structural details of PncA from *Pyrococcus horkoshii* (*10*) and *Acinetobacter baumanii* (*11*); however, no detailed kinetic analysis has been reported. Because of emerging antibiotic resistant strains of *M. tuberculosis*, a detailed understanding of the enzymatic activation of PZA is important. Moreover, a detailed mechanistic and structural understanding of all the enzymes involved in both the synthetic and salvage pathways of NAD^+ biosynthesis has the potential to produce novel targets for the development of therapeutics for the treatment of tuberculosis (*1*).

Previously, reported enzymatic activity assays for PncA involved end point assays, in which the enzymatic reaction was quenched at various time points and the mixture was separated by HPLC; the peaks for substrate and product are then integrated and compared to standards. We found this method both tedious and time-consuming and sought to develop a simple, spectroscopic enzymatic assay. Toward this end, we have developed a coupled enzymatic assay that allowed us to directly monitor the steady-state enzymatic activity of *M. tuberculosis* PncA (*Mt*PncA). Using this assay system, we have characterized aspects of the kinetics, mechanism, and inhibition by analogues of nicotinamide and pyrazinamide.

MATERIALS AND METHODS

Materials. All chemicals, buffers, salts, and L-glutamic dehydrogenase (GDH) were purchased from Sigma-Aldrich Chemical Co. (St. Louis, MO). All enzymes used for molecular biology were supplied by New England Biolabs (Ipswich, MA). PCR primers and *Escherichia coli* strain BL21(DE3) cells were obtained from Invitrogen (Carlsbad, CA). Deuterated water was obtained from Cambridge Isotope Laboratories (Andover, MA). DNA sequencing was performed by Genewiz (South Plainfield, NJ).

Cloning, Overexpression, and Purification of PncA. The open reading frame of Rv2043C (*pncA* gene) was amplified from *M. tuberculosis* H37Rv genomic DNA by standard PCR techniques

†This work was supported by National Institutes of Health Grant AI33696 (to J.S.B.).

*To whom correspondence should be addressed: Department of Biochemistry, Albert Einstein College of Medicine, 1300 Morris Park Ave., Bronx, NY 10461. Phone: (718) 430-3096. Fax: (718) 430-8565. E-mail: blanchar@aecom.yu.edu.

[1]Abbreviations: EDTA, ethylenediaminetetraacetic acid; GDH, L-glutamic dehydrogenase; HEPES, 4-(2-hydroxyethyl)-1-piperazineethanesulfonic acid; HPLC, high-performance liquid chromatography; IPTG, isopropyl β-D-thiogalactopyranoside; LB, Luria broth; MES, 2-(*N*-morpholino)ethanesulfonic acid; NADH, reduced nicotinamide adenine dinucleotide; Ni-NTA, nickel nitriloacetic acid; PCR, polymerase chain reaction; PncA, nicotinamidase; PZA, pyrazinamide; SDS−PAGE, sodium dodecyl sulfate−polyacrylamide gel electrophoresis; TAPS, *N*-tris(hydroxymethyl)methyl-3-aminopropanesulfonic acid; TB, tuberculosis; Tris, tris(hydroxymethyl)aminomethane.

© 2010 American Chemical Society

Scheme 1: NAD^+ Salvage (bottom) and de Novo (top) Pathways in *M. tuberculosis*

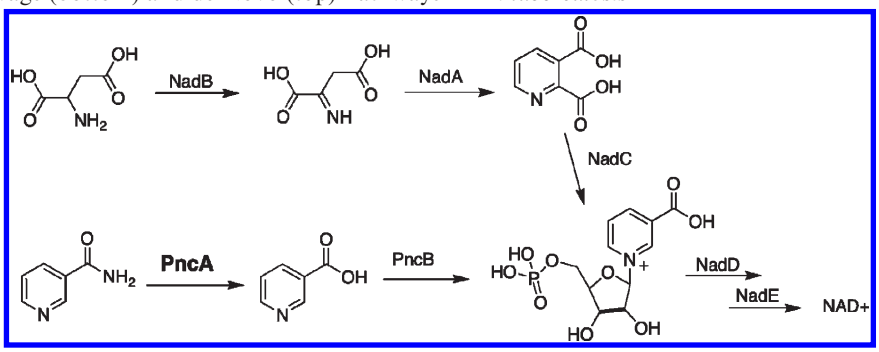

using the primers 5′-ATCCCGCTCATATGCGGCGTTGATCATCGTCGAC-3′ and 5′-ATCCCGCTCTCGAGTCAGGAGCTGCAAACCAACTCGAC-3′ containing the underlined *Nde*I and *Xho*I restriction sites, respectively. The PCR product was cloned into pET-28a(+), and the recombinant PncA was expressed in *E. coli* strain BL21(DE3). From a 100 mL overnight culture, 5 mL was used to inoculate 1 L cultures of LB medium supplemented with kanamycin (50 μg/mL). Cultures were grown to midlog phase ($A_{600} \sim 0.8$), cooled to 18 °C, induced with 0.5 mM IPTG, and further incubated overnight at 18 °C. Soluble expression of the protein was confirmed by sodium dodecyl sulfate–polyacrylamide gel electrophoresis (SDS–PAGE).

All protein purification steps were conducted at 4 °C. The cells were harvested by centrifugation at 6000*g*, resuspended in 50 mM HEPES (pH 7) containing 250 mM NaCl, 5 mM imidazole, protease inhibitors, and DNase I (0.1 μg/mL), and stirred for 30 min. The cells were lysed by sonication, and the cellular debris was removed by centrifugation at 18000*g* for 45 min. The supernatant was loaded by gravity flow onto a Ni-NTA column pre-equilibrated with resuspension buffer. The column was washed by gravity flow with 5 column volumes of wash buffer [50 mM Tris (pH 8.0) containing 250 mM NaCl and 60 mM imidazole]. Bound protein was eluted by gravity flow of 1.5–2 column volumes of 50 mM Tris (pH 8.0) containing 250 mM NaCl and 250 mM imidazole. The eluted protein was >95% pure as judged by SDS–PAGE, and further purification was judged to be unnecessary. The eluted protein was dialyzed overnight against 2 L of 30 mM HEPES (pH 7.5) containing 50 mM NaCl and stored at −20 °C.

Preparation of the H57D Mutant. Site-directed mutagenesis of the pET-28a(+) plasmid by standard PCR techniques was performed utilizing the primers 5′-GACCCGGGTGACGACTTCTCCGGCACA-3′ and 5′-TGTGCCGGAGAAGTCGTCACCCGGCTC-3′. The mutated plasmid was expressed and purified as described above. DNA sequencing analysis was performed by Genewiz.

Protein Estimation. The enzyme concentration was determined using an ε_{280} of 19940 M^{-1} cm^{-1} for native PncA. The concentration was also estimated by the Bio-Rad protein assay method using bovine serum albumin as a standard, and the two methods agreed favorably.

Measurement of Enzyme Activity by the Coupled Assay. Initial velocities for the reaction of *Mt*PncA were determined by monitoring the loss of absorbance at 340 nm associated with oxidation of NADH to NAD^+ by L-glutamic dehydrogenase (GDH) to produce glutamate from α-ketoglutarate. This reaction consumes one molecule of ammonia; therefore, the production of ammonia from the catalytic hydrolysis of nicotinamide or pyrazinamide by PncA is stoichiometric with NADH oxidation (Scheme 2). In a typical assay, 100 mM HEPES (pH 7.5) containing 5 mM α-ketoglutarate, 8 units of GDH, 200 μM NADH, and various concentrations of substrate (nicotinamide or pyrazinamide) were combined in a 1 mL cuvette. The reaction was initiated by addition of PncA, typically at a final concentration of 37.5 nM, and the decrease in absorbance at 340 nm was monitored at 25 °C for 8–10 min. Enzyme activities were calculated using the molar extinction coefficient of NADH (ε_{340} = 6220 M^{-1} cm^{-1}).

Scheme 2: Coupled Enzymatic Activity Assay Used for Spectrophotometric Observation of Steady-State PncA Kinetics

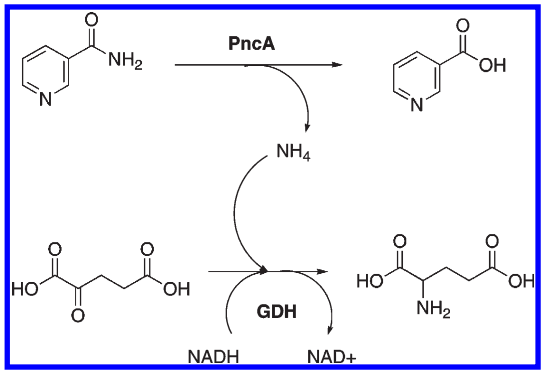

Measurement of Enzyme Activity with HPLC. We determined PncA activity by HPLC by applying the reaction mixture directly to a Mono Q anion exchange column and separating the substrate and product using a linear NaCl gradient. In a typical assay, 100 mM HEPES (pH 8.0) containing 100 μM nicotinamide and 37.5 nM PncA were combined at 25 °C. Addition of enzyme initiated the reaction, and at a specified time point, the reaction mixture was directly applied to an anion exchange column. A 100 mL NaCl gradient (from 0 to 1.2 M) afforded the separation of substrate and product, and the amount of conversion of nicotinamide by PncA was calculated via comparison of peak areas to authentic standards.

Dependence of PncA Activity on pH. The pH dependence of the kinetic parameters of PncA catalytic activity was determined using nicotinamide as the variable substrate. Activity was monitored every 0.5 pH unit from pH 5.0 to 9.5, using the following buffers: acetate for pH 5.0–5.5, MES for pH 5.5–6.7, HEPES for pH 6.7–8.0, and TAPS for pH 8.0–9.5. The kinetic parameters were determined using both spectrophotometric and HPLC assays.

pH Dependence of Inactivation by Iodoacetamide. A solution (100 μL final volume) containing 6 μM PncA in 100 mM phosphate buffer at various pH values was treated at

25 °C with 150 μM iodoacetamide. Aliquots (6 μL) were removed at various time points and added to a 1.0 mL solution containing 100 mM HEPES (pH 7.5), 5 mM nicotinamide, 5 mM α-ketoglutarate, 8 units of GDH, and 200 μM NADH. The enzyme activity was measured by monitoring the change in absorbance at 340 nm as described above. The rate of inactivation was measured over a pH range of 5.5−8.0, and the data were fit to the following equation using Prism

$$\log V = \log\{[Y_L + Y_H(K/H)]/(1 + K/H)\} \quad (1)$$

where V is the rate of inactivation, Y_L and Y_H are the pH-independent plateau values for the lower and upper regions, respectively, K is the ionization constant, and H is the hydrogen ion concentration.

Solvent Kinetic Isotope Effects. Solvent kinetic isotope effects on V and V/K were determined by measuring the initial velocity of amide cleavage by PncA at various concentrations of nicotinamide in either H_2O or 98% D_2O. The mixtures contained 100 mM HEPES (pH 8.0), nicotinamide (2.5−250 μM), 5 mM α-ketoglutarate, 8 units of GDH, 200 μM NADH, and 37.5 nM PncA. Assays were performed at 25 °C and were initiated by addition of PncA. Solvent deuterium isotope effects were fitted to the following equation:

$$V = (VA)/[KA(1 + F_i E_{V/K}) + A(1 + F_i E_V)] \quad (2)$$

where E_V and $E_{V/K}$ are the isotope effects on $k_{cat} - 1$ and $k_{cat}/K_m - 1$, respectively, F_1 represents the fraction of isotope (0.98), V is the maximal velocity, and A is the concentration of substrate.

Inhibition Studies with PncA. Several substrate analogues were tested as inhibitors of PncA using the coupled assay described above. In the case of the reversible inhibitors, initial velocities were measured while various concentrations of inhibitor were kept constant and the concentration of nicotinamide was varied (from 250 to 10 μM). Time courses for each inhibitor concentration were determined five times, and an average was calculated and used for subsequent data analysis. The time courses were fit to eq 3 for competitive inhibition kinetics:

$$\text{app}K_m = K_m(1 + I/K_I) \quad (3)$$

where appK_m is the apparent Michaelis−Menten constant, K_m is the true Michaelis−Menten constant, I is the concentration of the inhibitor, and K_I is the inhibitor dissociation constant.

In the case of the irreversible inhibitor pyrazinecarbonitrile (PCN), PncA (5 μM) was incubated in 30 mM HEPES (pH 7.5) containing 50 mM NaCl with various concentrations of PCN (10−25 μM), and at 0.5, 1, and 2 min, an aliquot was taken (6 μL) and the remaining PncA activity was determined spectrophotometrically with the coupled assay as described above. All measurements were performed in triplicate and compared to a control with no inhibitor. A Kitz−Wilson replot of the inactivation time course data was used to calculate the inactivation kinetic parameters.

RESULTS AND DISCUSSION

Cloning, Expression, and Purification. PCR amplification of the *pncA* gene of *M. tuberculosis* yielded a single fragment, and DNA sequencing confirmed the expected sequence and the absence of mutations introduced during PCR amplification. Overexpression of the PCR product yielded a protein with an apparent molecular mass in agreement with the expected mass (21 kDa) for *Mt*PncA, as judged by SDS−PAGE. Approximately 10 mg of purified enzyme was obtained per liter of culture. The enzyme was monomeric as judged by gel filtration of the purified protein.

Coupled Assay Development. To efficiently observe PncA catalytic activity, we utilized the catalytic activity of glutamate dehydrogenase (GDH), which converts α-ketoglutarate to glutamate, consuming one molecule of ammonia and oxidizing one molecule of NADH to NAD^+. The oxidation of NADH to NAD^+ produces a loss of absorbance at 340 nm, which can be easily monitored spectrophotometrically (Scheme 2). By using saturating concentrations of α-ketoglutarate and NADH and high concentrations of GDH, we were able to directly monitor the steady-state production of ammonia from the conversion of nicotinamide or pyrazinamide to their respective acids by PncA. To ensure that this assay was reliable, we compared the spectrophotometric, coupled assay with the fixed-time HPLC assay and demonstrated that similar kinetic constants were obtained with the two methods.

Determination of the Kinetic Parameters. Utilizing the coupled enzymatic assay, we determined the kinetic parameters of *Mt*PncA with both pyrazinamide and nicotinamide. With the natural substrate nicotinamide, we determined a K_m value of 14 ± 1 μM and a k_{cat} value of 3.1 ± 0.1 s^{-1}, corresponding to a k_{cat}/K_m value of 2.2×10^5 M^{-1} s^{-1}. In the case of pyrazinamide, we determined a K_m value of 300 ± 40 μM and a k_{cat} value of 3.8 ± 0.1 s^{-1}, corresponding to a k_{cat}/K_m value of 1.3×10^4 M^{-1} s^{-1}. It is important to note that these values are similar to those we determined with the previously mentioned end point HPLC assay. Also, PncA is extremely specific for nicotinamide and pyrazinamide, as we did not observe any enzymatic activity with benzamide or 6-aminonicotinamide.

Metal Ion Content. PncA from a number of sources is a divalent cation-dependent metalloenzyme reported to contain Mn^{2+}, Fe^{2+}, or Zn^{2+} (*8*, *10*). Our homogeneous preparations of the enzyme exhibited a distinct blue-green color at high concentrations (> 2 mg/mL). The metal ion in the *Mt*PncA appears to be tightly bound, and neither the addition of 5 mM EDTA nor reported inhibitory metals (Zn^{2+} for *Mt*PncA) resulted in any decrease in activity, although extensive dialysis versus EDTA has previously been reported to generate an apoenzyme that could be reconstituted with metal ion. In this report, the metal ion content of the *Mt*PncA was reported to include 0.44 and 0.47 mol of Mn^{2+} and Fe^{2+}, respectively, per mole of enzyme (*8*), and either Mn^{2+} or Fe^{2+} added to apo-*Mt*PncA could restore activity. When we performed EPR spectroscopy on our preparations, we observed a typical six-line spectrum indicating the presence of Mn^{2+} bound to the enzyme (data not shown). On the basis of the three-dimensional structures of the related *P. horikoshii* and *A. baumanii* nicotinamidases (*10*, *11*), and multiple-sequence alignment, the side chains of Asp49, His57, and His71 are the likely metal ion ligands in the *Mt*PncA active site. These nitrogen- and oxygen-containing ligands are commonly observed in metalloenzymes that bind either manganese or ferrous iron.

pH Dependence of the Kinetic Parameters. The pH dependence of the deamidase reaction was measured over the pH range of 5.0−9.5 using nicotinamide as the substrate. We did not observe any significant effect of pH on either the maximal velocity or the V/K_m value of nicotinamide. It is worth noting that care was taken to ensure the coupling enzyme, GDH, was present at sufficiently high concentrations to not be limiting across the pH range studied. Further, at several points across the pH range,

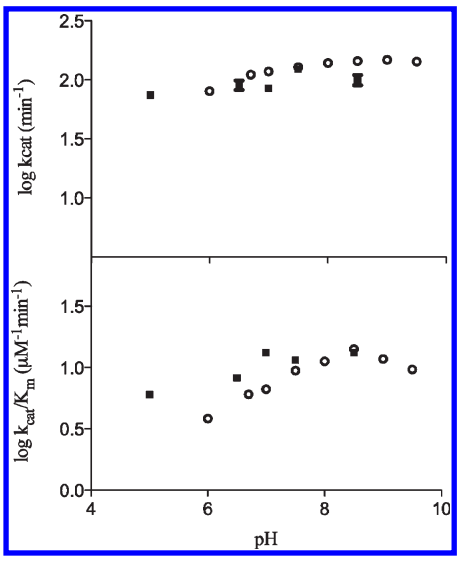

FIGURE 1: pH profile of PncA with nicotinamide as the substrate. Log k_{cat} vs pH (top) and log k_{cat}/K_m vs pH (below). All data points represent the mean of at least three separate sets of experiments. Black squares are values collected from the end point HPLC assay method, and white circles represent data collected with the enzyme-coupled assay method.

the kinetic parameters were determined using the end point HPLC assay, and the results were qualitatively equal at every point tested, as seen in Figure 1.

The lack of pH dependence for the amidase reaction is an intriguing result, as we had expected to see a pH dependence involving deprotonation of the active site cysteine (see below). Catalytic mechanisms proposed for PncA in the literature involve base-assisted attack by a nucleophilic cysteine on the carbonyl carbon of the substrate. This mechanism resembles the mechanisms proposed for the nitrilase superfamily of enzymes (*12*). The catalytic mechanism of nitrilases involves a nucleophilic cysteine, a lysine that stabilizes the tetrahedral intermediate, and a glutamate that acts as a general base catalyst (*12*). These residues most likely correspond to the conserved and essential Cys138, Lys96, and Asp8 residues in *M. tuberculosis* PncA and other nicotinamidases, where the glutamate is replaced with an aspartate. Therefore, the enzyme catalytic mechanism most likely involves the transfer of a proton from the cysteine thiol to the aspartate group, which has been previously proposed (*10*, *11*).

pH Dependence of the Inactivation by Iodoacetamide. Because PncA catalysis most likely involves a nucleophilic cysteine residue, we wanted to probe if the thiol-specific labeling agent, iodoacetamide, was an inactivator of PncA. Indeed, iodoacetamide was found to be an inactivator of PncA, and furthermore, incubation of PncA with iodoacetamide yielded a time- and concentration-dependent lost of enzymatic activity that was first-order over more than 30 min. The inactivation proved to be pH-dependent, as one can see in Figure 2. The inactivation rate was increased as the pH of the solution was increased from ~6 to 8, but at pH > 8, the rate of inactivation reached a plateau. Fitting the data to eq 1 revealed the change in the inactivation rate was due to a single ionizable group, with a pK value of 6.6, reflecting the pK of the active site, nucleophilic Cys138 in the free enzyme.

Solvent Kinetic Isotope Effects. Solvent kinetic isotope effects were determined by measuring the initial velocities in both H_2O and 98% D_2O at seven different concentrations of nicotinamide. These experiments were performed at pH 8.0, where

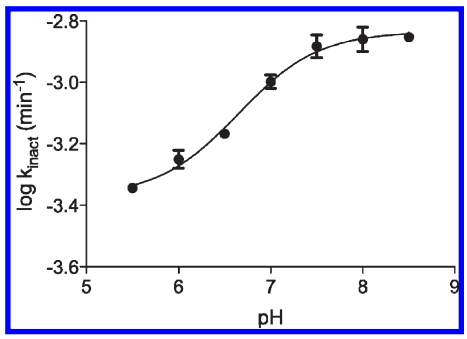

FIGURE 2: pH dependence of iodoacetamide inactivation of PncA. Dots represent experimentally determined values; the line represents a calculated fit as detailed in Materials and Methods.

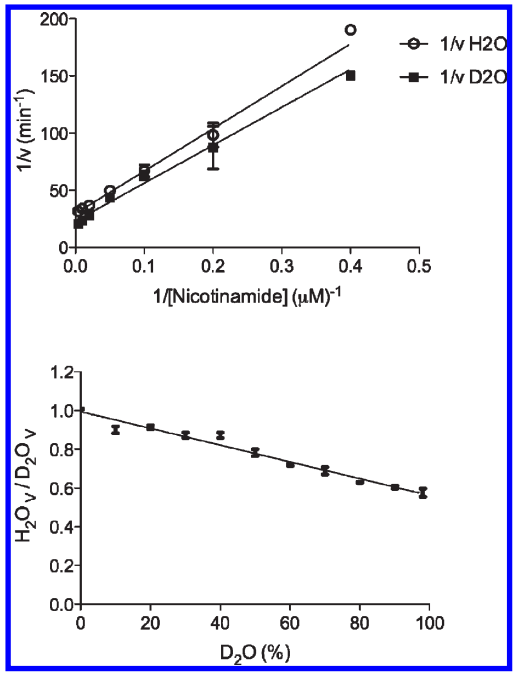

FIGURE 3: Solvent deuterium isotope effects. Circles and squares represent experimentally determined values [(○) in the presence of H_2O and (■) in the presence of 98% D_2O] (top). Proton inventory of the solvent kinetic isotope effects. Nicotinamide was used as the substrate under saturating conditions, and the amount of D_2O was varied from 0 to 98% (bottom).

both V and V/K were judged to be maximal and independent of pH. As Figure 3 reveals, ${}^{D_2O}k_{cat}$ was inverse, with a value of 0.64 ± 0.02. However, the solvent isotope effect did not have a statistically significant effect on k_{cat}/K_m, as it was determined to be 1.1 ± 0.1. Fractionation factors of most enzymatic groups that participate in acid−base chemistry are normal, or above 1. However, inverse solvent kinetic isotope effects are often associated with the participation of thiol groups in acid−base chemistry (*13*, *14*). Thiols are known to exhibit inverse fractionation factors (solvent equilibrium isotope effects) in the range of 0.4−0.6 (*13*), and we suggest the inverse fractionation factor of the catalytic cysteine of *Mt*PncA is responsible for the inverse solvent kinetic isotope effect on k_{cat}, as the nucleophilic thiolate anion is required for attack on the carbonyl carbon of nicotinamide.

A proton inventory was performed to determine the proton multiplicity that is present in the solvent kinetic isotope effect. The proton inventory was determined under saturating conditions of nicotinamide, and the percent of D_2O was varied from 0

Scheme 3: Proposed Mechanism of Catalysis of *Mt*PncA

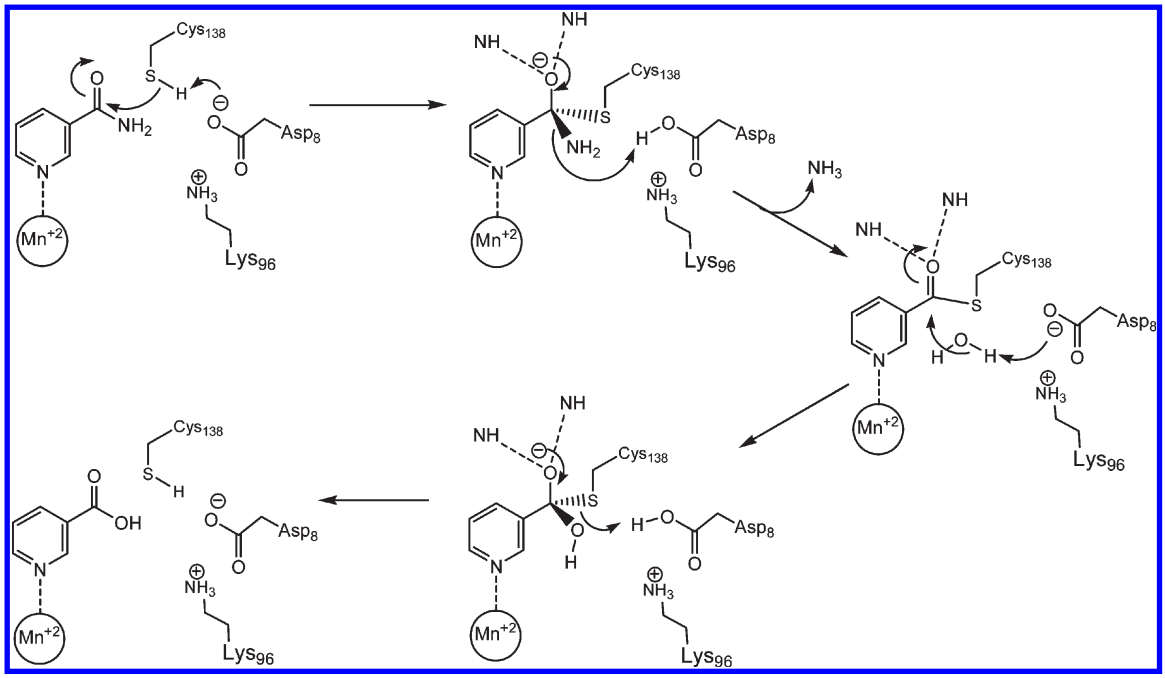

to 98% in increments of 10%. As shown in the bottom panel of Figure 3, the linearity exhibited by the proton inventory demonstrates that one proton is being transferred in the isotopically sensitive step, and the negative slope confirms the inverse nature and magnitude of the solvent kinetic isotope effect observed on k_{cat}.

Comparing Mycobacterium bovis PncA. *M. bovis* expresses a *pncA* gene that contains a single mutation resulting in an aspartic acid replacing His57 of PncA (H57D). Further, *M. bovis* has been shown to be innately resistant to treatment by pyrazinamide. His57 has been proprosed to be directly involved in metal binding of the Mn^{2+} in several PncA's for which three-dimensional structures are known, and literature reports that this mutant is unable to bind metal. This results in a substantial decrease in enzymatic activity, although to the best of our knowledge, the kinetic properties of *M. bovis* PncA have not yet been reported. Toward this end, we employed site-directed mutagenesis to express and purify the H57D mutant as detailed in Materials and Methods. As expected, we observed a loss of the Mn^{2+} signal in the EPR spectrum of the H57D mutant (data not shown). The mutant is not, however, completely inactive. With nicotinamide as the substrate, we determined the K_m value to be $13 \pm 2\ \mu$M and the k_{cat} value to be $0.50 \pm 0.01\ s^{-1}$, corresponding to a k_{cat}/K_m value of $3.7 \times 10^4\ M^{-1}\ s^{-1}$. This represents a 6-fold decrease in the observed catalytic turnover of the substrate by the mutant, but interestingly, we did not observe a change in the K_m for nicotinamide. Using the substrate pyrazinamide, we determined a K_m value to be $16 \pm 4\ \mu$M and a k_{cat} value of $0.10 \pm 0.01\ s^{-1}$, corresponding to a k_{cat}/K_m value of $6.2 \times 10^3\ M^{-1}\ s^{-1}$. For pyrazinamide, both the K_m value and the k_{cat} value have been decreased 20- and 38-fold, respectively, for the H57D mutant. The 38-fold decrease in k_{cat} for pyrazinamide is likely enough to account for the resistance of *M. bovis* to the bactericidal effects of pyrazinamide.

Catalytic Mechanism of PncA. There has been some disagreement in the literature about the catalytic mechanism of PncA. The earliest mechanistically relevant report came from Du et al. (*10*), who reported the crystal structure of the *P. horikoshii* nicotinamidase (*Ph*PncA). The overall structure was most similar to that of *N*-carbamoylsarcosine amidohydrolase from *Arthrobacter* sp. and contained the active site catalytic triad of conserved residues (Cys133, Arg84, and Asp19). Further, they found the protein was a monomer and the active site contained a Zn^{2+} ion. On the basis of the crystal structure, Du et al. proposed a mechanism that involves nucleophilic attack by the active site Cys to form a tetrahedral intermediate and subsequent loss of ammonia that yields an acyl intermediate. Hydrolysis was proposed to occur by the subsequent attack from a Zn^{2+}-bound hydroxide ion to give the free enzyme and product.

Following this initial report, Zhang et al. reported a characterization of *M. tuberculosis* nicotinamidase (*Mt*PncA) (*8*). They found *Mt*PncA to be a monomer, and the protein contained Mn^{2+} or Fe^{2+} in an approximate 0.5:0.5 molar ratio. Zinc did not restore amidase activity when incubated with the apoenzyme and was also inhibitory to the wild-type enzyme. Site-directed mutagenesis of several residues of *Mt*PncA showed that the triad of Cys138, Asp8, and Lys96 was essential for catalytic activity, as the mutants C138A, D8A, and K96A completely lost amidase activity but retained the ability to bind metal. Further, Asp49, His51, His57, and His71 were deemed likely to be directly involved in metal binding as mutation of any of these residues caused the complete loss of metal from the protein.

Most recently, Fyfe et al. reported the crystal structure of *A. baumanii* PncA (*Ab*PncA) and found it to be a dimer that contained either Fe^{2+} or Zn^{2+} in a roughly 0.5:0.5 molar ratio (*11*). They proposed a mechanism of catalysis that involves nucleophilic attack of the active site cysteine that is aided by stabilization of the tetrahedral intermediate by an oxyanion hole formed from the backbone amides of Cys159 and Ala155 (*Ab*PncA numbering). Asp16 was proposed to deprotonate Cys159 to initiate catalysis and to donate a proton to aid the release of NH_3 during the tetrahedral intermediate collapse to form the thioester acyl intermediate. Water is then activated by proton abstraction by Asp16 for nucleophilic attack on the covalent acyl−enzyme intermediate to yield a thiolate and nicotinic acid. Transfer of a proton from Asp16 to the active site cysteine completes the catalytic cycle.

On the basis of our data, we propose the catalytic mechanism of *M. tuberculosis* PncA is most similar to the mechanism recently proposed for *Ab*PncA. As one can see in Scheme 3, the catalytic mechanism involves an initial proton equilibrium between Cys138 and the ionized Asp8, yielding the nucleophilic thiolate that attacks the carbonyl of the amide substrate to produce a tetrahedral intermediate. The ionization state of Asp8 is very likely to be strongly influenced by the adjacent Lys96. This first step is clearly the one that is reported by the inverse solvent kinetic isotope effect on k_{cat}. In the free enzyme, the p*K* value of Cys138 (or more appropriately the Cys138−Asp8 pair) is close to 6.6. However, when the substrate binds, the ionization behavior of these residues is substantially altered, causing the p*K* value to shift downward, and out of the experimentally accessible range. Even at the lower pH extremes, only a small decrease in k_{cat} is observed.

In the second step, the productive collapse of the tetrahedral intermediate is assisted by protonation of the amine to generate ammonia and the covalent Cys138 thioester. The departing ammonia is replaced with a water molecule, which is activated for attack on the thioester by the ionized carboxylate of Asp8. Reaction of water with the thioester generates the second tetrahedral intermediate, which in the final step decomposes to generate the final aryl carboxylic acid product. Productive decomposition is again facilitated by the transfer of a proton from the protonated carboxyl of Asp8, regenerating the active site residues in their original ionization state.

Table 1: Inhibition Constants for PncA of Several Structural Analogues

Inhibitor	K_i (μM)
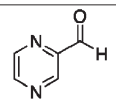	1.5 ± 0.7
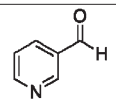	0.3 ± 0.1
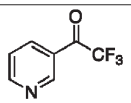	420 ± 100
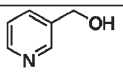	63 ± 31
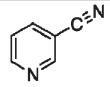	140 ± 14
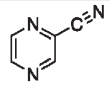	k_{inact} = 0.06 ± 0.01 sec^{-1} K_i = 61 ± 3 μM

Inhibition of PncA. It has been well established that current antitubercular drugs have either a reduced or a minimal effect on latent, nonreplicating bacilli, which leads to long treatment therapy and contributes to the appearance of multiple drug-resistant strains (*1*, *15*). It has been reported that the NAD^+ salvage pathway is upregulated in *M. tuberculosis* under conditions of hypoxia (*1*). Inhibition or disruption of both the NAD^+ salvage and de novo pathways is an interesting option for targeting both active and latent tuberculosis.

Toward this end, we performed a screen of nicotinamide analogues to search for possible inhibitors of PncA. As shown in Table 1, the screen resulted in several competitive inhibitors with inhibition constants in the micromolar to submicromolar range. The most potent inhibitor, 3-pyridine carboxaldehyde, exhibited a K_i value of 290 nM. All of the inhibitors tested were reversible, competitive inhibitors, with one exception. Unlike the other inhibitors, pyrazinecarbonitrile (PCN) is an irreversible inactivator of PncA. Incubation of the enzyme with PCN resulted in a time- and concentration-dependent loss of enzymatic activity (Figure 4, left), and enzymatic activity is not restored upon removal of excess inactivator or prolonged dialysis. A Kitz−Wilson replot of the inactivation data (Figure 4, right) gave a k_{inact} of 0.06 ± 0.01 s^{-1}, and a K_i of 61 ± 3 μM. This gives an apparent second-order rate constant for the inactivation of the enzyme by PCN (k_{inact}/K_i) of 975 M^{-1} s^{-1}. Interestingly, the nicotinamide analogue of PCN, 3-pyridinecarbonitrile, is a reversible, competitive inhibitor of PncA with a K_i of ∼100 μM. Neither compound is a substrate for the enzyme. Given the conserved nature of the catalytic residues in deamidases, such as nicotinamidase, and bona fide nitrilases in the nitrilase superfamily, it is curious that PCN is an irreversible inactivator of PncA. Nitrilases use the catalytic cysteine to attack the carbon atom of the cyano group, generating initially the thioimine, which upon hydrolysis yields the thioester, an intermediate in both reactions. The mechanism by which PCN inactivates the enzyme is currently under investigation, as is the compound's ability to inhibit NAD^+ biosynthesis in microorganisms.

Conclusion. *M. tuberculosis* is responsible for more deaths worldwide than any other bacterial infection (*16*). It is therefore important to expand our understanding of the activation of the front-line antibiotic, pyrazinamide, as well as to improve our understanding of the NAD^+ salvage pathway. This work provides a detailed examination of the chemical and kinetic

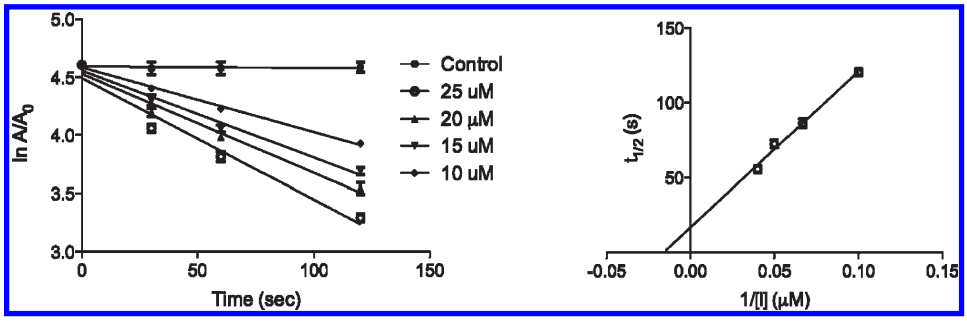

FIGURE 4: Semilog plot of the time courses for the inactivation of PncA with various concentrations of pyrazine carbonitrile (left). Kitz−Wilson replot of the inactivation data (right).

mechanism of PncA, the amidase that is serendipitously responsible for the activation of a major TB therapeutic drug, pyrazinamide. The NAD^+ salvage and de novo pathways are essential to both latent and active TB, and efforts to develop new therapeutics that target enzymes in these pathways in *M. tuberculosis* are emerging.

ACKNOWLEDGMENT

We sincerely thank Dr. Gary J. Gerfen for help with the EPR experiments.

REFERENCES

1. Boshoff, H. I. M., Xu, X., Tahlan, K., Dowd, C. S., Pethe, K., Camacho, L. R., Park, T.-H., Yun, C.-S., Schnappinger, D., Ehrt, S., Williams, K. J., and Barry, C. E. (2008) Biosynthesis and Recycling of Nicotinamide Cofactors in *Mycobacterium tuberculosis*. *J. Biol. Chem. 283*, 19329–19341.
2. Sheen, P., Ferrer, P., Gilman, R., Lopez-Llano, J., Furentes, P., Valencia, E., and Zimic, M. (2009) Effect of pyrazinamidase activity on pyrazinamide resistance in *Mycobacterium tuberculosis*. *Tuberculosis 89*, 109–113.
3. Zhang, Y., and Mitchison, D. (2003) The curious characteristics of pyrazinamide: A review. *Int. J. Tuberc. Lung Dis. 7*, 6–21.
4. Lemaitre, N., Sougakoff, W., Truffot-Pernot, C., and Jarlier, V. (1999) Characterization of new mutations in pyrazinamide-resistant strains of *Mycobacterium tuberculosis* and identification of conserved regions important for the catalytic activity of the pyrazinamidase PncA. *Antimicrob. Agents Chemother. 43*, 1761–1763.
5. Yuksel, P., and Tansel, O. (2009) Characterizaiton of pncA mutations in pyrazinamide-resistant *Mycobacterium tuberculosis* in Turkey. *New Microbiol. 32*, 153–158.
6. Pandey, S., Newton, S., Upton, A., Roberts, S., and Drinkovic, D. (2009) Characterisation of pncA mutations in clinical *Mycobacterium tuberculosis* isolates in New Zealand. *Pathology 41*, 582–584.
7. Zhang, H., Bi, L., Li, C., Sun, Z., Deng, J., and Zhang, X. (2009) Mutations found in the pncA gene of *Mycobacterium tuberculosis* in clinical pyrzainamide-resistant isolates from a local region of China. *J. Int. Med. Res. 37*, 1430–1435.
8. Zhang, H., Deng, J., Bi, L., Zhou, Y., Zhang, Y., Zhang, C., Zhang, Y., and Zhang, X. (2008) Characterization of *Mycobacterium tuberculosis* nicotinamidase/pyrazinamidase. *FEBS J. 275*, 753–762.
9. Zimhony, O., Cox, J., Welch, J., Vilcheze, C., and Jacobs, W. (2000) Pyrazinamide inhibits the eukaryotic-like fatty acid synthetase I (FASI) of *Mycobacterium tuberculosis*. *Nat. Med. 6*, 1043–1047.
10. Du, X., Wang, W., Kim, R., Yakota, H., Nguyen, H., and Kim, S.-H. (2001) Crystal Structure and Mechanism of Catalysis of a Pyrazinamidase from *Pyrococcus horikoshii*. *Biochemistry 40*, 14166–14172.
11. Fyfe, P. K., Rao, V. A., Zelma, A., Cameron, S., and Hunter, W. N. (2009) Specificity and Mechanism of *Acinetobacter baumanii* Nicotinamidase: Implications for Activation of the Front-Line Tuberculosis Drug Pyrazinamide. *Angew. Chem., Int. Ed. 48*, 9176–9179.
12. Thuku, R. N., Brady, D., Benedik, M. J., and Sewell, B. T. (2009) Microbial nitrilases: Versatile, spiral forming, industrial enzymes. *J. Appl. Microbiol. 106*, 703–727.
13. Quinn, D. M., and Sutton, L. D. (1991) in Enzyme mechanism from isotope effects (Cook, P. F., Ed.) pp 73−126, CRC Press, Boca Raton, FL.
14. Sikora, A. L., Frankel, B. A., and Blanchard, J. S. (2008) Kinetic and Chemical Mechanism of Arylamine N-Acetyltransferase from *Mycobacterium tuberculosis*. *Biochemistry 47*, 10781–10789.
15. Gomez, J. E., and Mckinney, J. D. (2003) *M. tuberculosis* persistence, latency, and drug tolerance. *Tuberculosis 84*, 29–44.
16. Dye, C., Scheele, S., Dolin, P., Pathania, V., and Raviglione, M. C. (1999) Global Burden of Tuberculosis: Estimated Incidence, Prevalence, and Mortality by Country. *J. Am. Med. Assoc. 282*, 677–686 (the World Health Organization Global Surveillance and Monitoring Project).